Journal Pre-proof

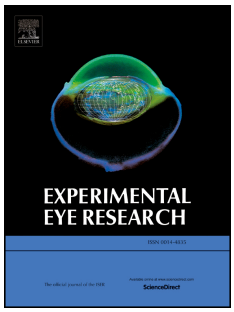

Peptide-based immunotherapy against oxidized elastin ameliorates pathology in mouse model of smoke-induced ocular injury

Bärbel Rohrer, Nathaniel Parsons, Balasubramaniam Annamalai, Crystal Nicholson, Elisabeth Obert, Bryan Jones, Andrew D. Dick

PII: S0014-4835(21)00321-3

DOI: https://doi.org/10.1016/j.exer.2021.108755

Reference: YEXER 108755

To appear in: *Experimental Eye Research*

Received Date: 8 June 2021

Revised Date: 24 August 2021

Accepted Date: 30 August 2021

Please cite this article as: Rohrer, Bä., Parsons, N., Annamalai, B., Nicholson, C., Obert, E., Jones, B., Dick, A.D., Peptide-based immunotherapy against oxidized elastin ameliorates pathology in mouse model of smoke-induced ocular injury, *Experimental Eye Research* (2021), doi: https://doi.org/10.1016/j.exer.2021.108755.

Peptide-based immunotherapy against oxidized elastin ameliorates pathology in mouse model of smoke-induced ocular injury.

(Running header: Peptide immunotherapy reduces ocular pathology)

Bärbel Rohrer[1,2,3*], Nathaniel Parsons[1], Balasubramaniam Annamalai[1], Crystal Nicholson[1], Elisabeth Obert[1], Bryan Jones[4] and Andrew D. Dick[5].

Departments of [1]Ophthalmology and [2]Neurosciences Division of Research, Medical University of South Carolina, Charleston, South Carolina, United States of America; [3]Ralph H. Johnson VA Medical Center, Division of Research, Charleston, SC 29401, United States of America; [4]Department of Ophthalmology, University of Utah, Salt Lake City, UT 84132, United States of America; and [5] University of Bristol, Bristol BS8 1TD and University College London-Institute of Ophthalmology and the National Institute for Health Research Biomedical Research Centre, Moorfields Eye Hospital, London EC1V 9EL, UK.

*Corresponding Author

BR: Department of Ophthalmology, Medical University of South Carolina, 167 Ashley Avenue, Charleston, SC 29425; phone: (843) 792-5086; fax (843) 792-1723; e-mail: rohrer@musc.edu.

Keywords: age-related macular degeneration, elastin, peptide-based immunotherapy, complement, smoking

Number of words, main text (excluding references and figure legends): 5211
Number of words, abstract: 239
Number of Figures: figures 6 Number of Tables: 0
Supplemental Material: figures and videos: 2 figures

ABSTRACT

Purpose: Age-related macular degeneration (AMD), the leading cause of blindness in western populations, is associated with an overactive complement system, and an increase in circulating antibodies against certain epitopes, including elastin. As loss of the elastin layer of Bruch's membrane (BrM) has been reported in aging and AMD, we previously showed that immunization with elastin peptide oxidatively modified by cigarette smoke (ox-elastin), exacerbated ocular pathology in the smoke-induced ocular pathology (SIOP) model. Here we asked whether ox-elastin peptide-based immunotherapy (PIT) ameliorates damage.

Methods: C57BL/6J mice were injected with ox-elastin peptide at two doses via weekly subcutaneous administration, while exposed to cigarette smoke for 6 months. $Fc\gamma R^{-/-}$ and uninjected C57BL/6J mice served as controls. Retinal morphology was assessed by by electron microscopy, and complement activation, antibody deposition and mechanisms of immunological tolerance were assessed by Western blotting and ELISA.

Results: Elimination of Fcγ receptors, preventing antigen/antibody-dependent cytotoxicity, protected against SIOP. Mice receiving PIT with low dose ox-elastin (LD-PIT) exhibited reduced humoral immunity, reduced complement activation and IgG/IgM deposition in the RPE/choroid, and largely a preserved BrM. While there is no direct evidence of ox-elastin pathogenicity, LD-PIT reduced IFNγ and increased IL-4 within RPE/choroid. High dose PIT was not protective.

Conclusions: These data further support ox-elastin role in ocular damage in SIOP in part via elastin-specific antibodies, and support the corollary that PIT with ox-elastin attenuates ocular pathology. Overall, damage is associated with complement activation, antibody-dependent cell-mediated cytotoxicity, and altered cytokine signature.

PRECIS: Elastin-degradation in BrM in smoke-exposed mice is associated with generation of anti-elastin antibodies that bind to RPE-BrM, triggering complement activation. Treatment with smoke-modified elastin peptide reduces structural and functional damage, suggesting that AMD might be preventable.

INTRODUCTION

Age-related macular degeneration (AMD), which occurs in two forms, wet and dry (Brown et al., 2005), is diagnosed as a loss of central vision alongside classical clinical features of drusen and retinal pigment epithelium (RPE) disturbance. Loss of function results from damage to macular photoreceptors and structural damage in both forms is associated with pathology at the RPE/choroid interface.

We have previously focused on the potential role of the middle elastic layer (EL) of Bruch's membrane (BrM) in initiation and progression of disease. The EL together with the other layers of BrM undergoes age-related changes. The most obvious change is the thickening with aging and disease across both the peripheral and the macular BrM, that is linked to lipid buildup (Curcio et al., 2011), although the macula changes occur more rapidly (Johnson et al., 2007). The middle EL is made up collagen VI, fibronectin, and other proteins surrounding a layer of cross-linked linear elastin fibers (Curcio and Johnson, 2013). Relevant for the context of AMD, the structural integrity as well as the width of the EL is less in the macula than in the periphery; and in eyes with early AMD and active choroidal neovascularization (CNV), this difference is ever more pronounced (Chong et al., 2005). Elastin endows tissues and extracellular matrices with long-range elasticity necessary for their physiological functions. For BrM's properties, this means that with aging, its biomechanical properties and that its ability to prevent the invasion of blood vessels might be impaired, potentially provides some rationale why CNV occurs in this anatomical location (Chong et al., 2005). Of note, probably one of the earliest suggestions of impaired elastin physiology in AMD came from Blunkenkranz and coworkers, who suggested "that generalized increased susceptibility of elastic fibers to photic or other degenerative stimuli

is a new and important risk factor for choroidal neovascularization" (Blumenkranz et al., 1986). Interestingly, it has been reported that AMD patients have elevated concentrations of elastin-peptide in serum (Sivaprasad et al., 2005), together with elevated levels of circulating elastin IgG and IgM autoantibodies (Morohoshi et al., 2012b), and elevating serum elastin fragments in mouse increased expression and deposition of collagen IV in the RPE/choroid complex (Skeie et al., 2012). Anti-elastin B- and T-cell immunity has also been observed in other diseases such as chronic obstructive pulmonary disease (Rinaldi et al., 2012), together with skin elastin degradation (Maclay et al., 2012) and the presence of elastin degradation products in urine (Stone et al., 1995). Finally, HTRA1 is an elastase-like enzyme (Jones et al., 2011) and HTRA1 variants confer similar risk to wet and dry AMD (Cameron et al., 2007). In RPE cells with heterozygous risk 10q26 allele increased expression of HTRA1 and extracellular matrix proteins has been demonstrated, (Lin et al., 2018) making HTRA1 another target for treatment (Tom et al., 2020). Based on these observations we have previously postulated that abnormalities in elastin homeostasis together with antibody production may play a role in AMD progression (Annamalai et al., 2020).

Antibodies produced in response to neo-proteins or modified self protein epitopes are of both IgG or IgM antibody class and may correspond with the generation of both B and T cell memory. In the context of AMD, antibodies are of great interest, since they may be directly cytotoxic, are one of the main activators of the complement system, and bind to Fc receptors eliciting further immune activation.

The complement system is an essential part of the evolutionarily ancient innate immune system. Its main role is to eliminate foreign antigens and pathogens as part of the normal host response; but excessive complement activation is also involved in the pathogenesis disease states, including AMD (reviewed in (Holers, 2003)). The complement system can be activated by three distinct pathways: the classical (CP), lectin (LP) and alternative pathway (AP) (Muller-Eberhard, 1988), with IgG and IgM antibodies participating in the activation of both the CP and LP. This can lead to the generation of an inflammatory environment by generating anaphylatoxins or membrane-attack-complex formation and direct cell injury (complement-dependent cytotoxicity; CDC). In addition, antibodies (IgG, IgA or IgE) bound to their respective antigens on surfaces can engage Fcγ-receptors (FcγR) on immune effector cells to trigger antibody-dependent cell-mediated cytotoxicity (ADCC) (Saeed et al., 2017).

We have tested the hypothesis of the involvement of anti-elastin antibodies in RPE/BrM damage in a mouse model of ocular damage with features of human dry AMD, the smoke-induced ocular pathology (SIOP) model (Woodell et al., 2013). We have shown that long-term smoke exposure in C57BL/6J mice reduces ERG response amplitudes and contrast sensitivity, and leads to structural changes in RPE/BrM, including a thickening of BrM and a loss of the EL (Woodell et al., 2013). Pathology was found to be dependent on the activation of the AP (Woodell et al., 2013; Woodell et al., 2016). As follow-up experiments, we asked if excessive anti-elastin antibody production would increase complement activation to exacerbate SIOP. In the SIOP model, we showed that immunization with a cigarette smoke modified form of elastin (ox-elastin) led to the generation of IgG and IgM antibodies, leading to more pronounced vision loss, thicker BrM and more damaged RPE mitochondria when compared to non-immunized mice, or

those immunized with a control elastin peptide. Pathology was correlated with increased levels of IgM, IgG3 and IgG2b together with C3 activation or C3 breakdown products in RPE/choroid fraction of the mice. Based on these experiments we speculated that in the SIOP model, antibodies generated de-novo against ox-elastin (IgG) bound to ox-elastin generated by smoke in BrM might generate cytotoxicity and inflammation. Inflammation might be generated by antibodies activating complement via the classical or lectin pathway leading to complement-dependent cytotoxicity (CDC) or ADCC. In support of CDC in SIOP pathology, Wang and colleagues have documented C3a, C5, C5b-9 and CFH deposition in the area of BrM, (Wang et al., 2009) and our work demonstrated localization of the complement activation prodect C3d in RPE/BrM and choroid after smoke exposure, with pathology ameliorated in complement factor B knockout mice (Woodell et al., 2013). Hence, first we asked whether in addition to their role in CDC, antibodies might regulate pathology in this model through interacting with Fc receptors. And second, given this data, albeit with only indirect evidence of ox-elastin induced pathology, here we asked whether antibody-mediated damage in the SIOP model could be blunted by peptide-based therapy against the ox-elastin peptide.

MATERIAL AND METHODS

Animals. C57BL/6J and were purchased (Jackson Laboratory, Bar Harbor, ME) and maintained as breeding colonies. Fcγ receptor γ chain–deficient mice were generously shared by Dr. Carl Atkinson and represent mice purchased from Taconic Farm (Fcer1g - model 583) backcrossed 12 generations onto the C57BL/6J background (Elvington et al., 2012). Mice were housed under a 12:12 h, light:dark cycle with access to food and water ad libitum. All experiments were

147 approved by the Medical University of South Carolina Institutional Animal Care and Use
148 Committee and performed in accordance with the Association for Research in Vision and
149 Ophthalmology statement for the use of animals in ophthalmic and vision research. The
150 observers were masked to the treatment of the animals.
151
152 To investigate the impact of PIT, mice were injected weekly via subcutaneous route with 1 (low
153 dose; LD) or 10 μg (high dose; HD) of smoke-oxidized mouse lung elastin peptides (Elastin
154 Products Company, Owensville MO). 10 μg of peptide was used in the immunization paradigm
155 (Annamalai et al., 2020), and was chosen as the high dose; 1 μg of peptide was selected for the
156 low concentration, a dose of peptide efficacious in controlling symptoms of lupus in a mouse
157 model (Kang et al., 2005). Cigarette smoke modified elastin peptides (termed oxidized elastin, or
158 ox-elastin) were generated as published previously (Annamalai et al., 2020). In short, mouse
159 lung elastin peptides at 1 mg/mL in PBS (pH 6.4), were incubated in 10% cigarette smoke
160 extract (Kunchithapautham et al., 2014) for 24 hrs at 37°C, followed by dialysis (ThermoFisher).
161 A control cohort received PBS injections.
162
163 *Exposure to Cigarette Smoke.* Cigarette smoke exposure was carried out according to our
164 published protocol (Woodell et al., 2013), exposing animals to cigarette smoke using the Teague
165 TE-10 total body smoke exposure system (Teague Enterprises, USA) for 5 hours per day, 5 days
166 per week for 6 months, using 3R4F reference cigarettes (University of Kentucky, Louisville,
167 KY).
168

169 *ELISA assays.* ELISA assays were performed as described in detail previously (Annamalai et al.,
170 2020). Microtiter (Immulon2; Dynatech Laboratories, Chatilly, VA) plates were coated with 10
171 μg/mL cigarette smoke modified mouse lung elastin peptides, washed, blocked with 3% milk in
172 PBS, followed by exposure to increasing doses of mouse serum (1:100 to neat) and probed with
173 anti-mouse secondary antibodies (anti-IgG, G1 and G2a andanti-IgM) coupled to peroxidase and
174 color development using Turbo-TMB ELISA (Pierce; Thermo Scientific, Rockford, IL).

175

176 *Western Analysis.* Mouse RPE/choroid/sclera (from herein referred to as RPE/choroid fraction)
177 preparations were extracted and equal amounts of protein were loaded per lane on 4-20 %
178 Criterion™ TGX™ precast gels (Bio-Rad Laboratories, Inc.) as described previously
179 (Annamalai et al., 2020). Separated samples were transferred to PVDF membranes, incubated in
180 primary antibody followed by appropriate secondary antibodies coupled to peroxidase, followed
181 by band development and detection using Clarity™ Western ECL blotting substrate (Bio-Rad
182 Laboratories, Inc.) and chemiluminescent detection. Protein bands were scanned and densities
183 quantified using ImageJ software. The following antibodies were used: anti-C3d (clone 11)
184 (Thurman et al., 2013), anti-mouse IgG and IgM (Santa Cruz Biotechnology), anti-TGFβ, IL4,
185 IL-10 and IFNγ; and all blots were normalized to beta-actin (Cell Signaling Technology).

186

187 *Electron microscopy*
188 Tissue preparation and ultrastructural analysis were performed as described before (Thurman et
189 al., 2013). In short, eyes were immersion fixed in 2.5% glutaraldehyde, 1% formaldehyde, 3%
190 sucrose, and 1 mM MgSO4 in 0.1 M phosphate buffer, pH 7.4. A small central, nasal portion

corresponding to the site analyzed by OCT was osmicated, en-bloc staining with uranyl acetate, dehydrated in graded ethanols, resin embedded (Woodell et al., 2013) and sectioned (90 nm) using a Leica Ultramicrotome, collecting the sections onto carbon-coated Formvar® films supported by nickel slot-grids.

Electron microscopic (EM) images were captured using a JEOL JEM 1400 transmission electron microscope using SerialEM software for automated image capture. Datasets (1200–1500 images per section) were used generate image mosaics (NCR Toolset) that were evaluated by Adobe Photoshop (Adobe Systems, San Jose, CA, USA) and ImageJ (http://imagej.nih.gov/ij/; provided in the public domain by the National Institutes of Health, Bethesda, MD, USA) software. The percent damaged BrM was determined based on the evaluation of BrM thickness along multiple ~25 μm length sections per sample, considering the thickness exceeding 0.28 μm as damaged (a normal BrM in age-matched room air exposed mice has a thickness of 0.22 ± 0.04 μm). The mask overlying BrM to be analyzed was previously published by us in the same animal model (Annamalai et al., 2020). Within damaged stretches of thickened BrM, the size (i.e., length along BrM) and area of the deposits were assessed along multiple 10 μm length sections, resulting in a single value per mouse. Overall, this approach, which we have used before (Woodell et al., 2013; Woodell et al., 2016), has high statistical power as it analyzes a large portion of randomly selected regions of BrM per eye.

Statistics

Data are reported as the mean ±SEM. Data consisting of repeated measures were analyzed with a repeated measures ANOVA (accepting a significance of $P<0.05$) followed by an ANOVA with

Bonferroni correction correcting for multiple comparisons; data consisting of multiple groups but single measurements, by a one-way ANOVA (accepting a significance of $P<0.05$), followed by Student's t-tests for individual comparisons; and data differing from control value were analyzed by *Z*-test (StatView, SAS Institute, Inc., Cary, NC).

RESULTS

Elimination of Fcγ receptor prevents SIOP damage based on histology and visual function analysis

IgGs/IgMs bound to ligands on cell surfaces, basement membranes or extracellular matrices can participate in inflammation via two distinct mechanisms, CDC and ADCC. CDC involves the activity of anaphylatoxins and the generation of C5b-9, ADCC involves activation of target cells via Fcγ receptors. Fcγ receptor activation can contribute to damage in several ways. Fcγ receptors on effector cells recruited to affected tissues possibly by anaphylatoxins, can bind to IgGs bound to antigens in tissues, resulting in ADCC. Alternatively, Fcγ receptor activation has been shown to contribute to the maintenance of peripheral tolerance (Desai et al., 2007). Here we asked whether Fcγ receptor γ chain–deficient mice mice are susceptible to smoke-induced ocular pathology and vision loss. After 6 months of smoke, contrast threshold in control and smoke exposed $Fc\gamma R^{-/-}$ mice was identical (**Fig. 1A**), as was the thickness of BrM (**Fig. 1B**) or the structure of the basolaminar infoldings (**Fig. 1C**) as assessed by electronmicroscopy (**Fig. 1D**). While these data do not exclude an effect of Fcγ receptor activation on maintenance of peripheral tolerance, that effect could not be assessed in these animals as the effect on ADCC was

predominant. Taken together, both CDC (Woodell et al., 2013; Woodell et al., 2016) and ADCC seem to play a role in SIOP, activated in part via elastin-specific antibodies.

Peptide-based immunotherapy with ox-elastin reduces smoke-induced ocular pathology in mouse

We have shown previously that C57B/6J mice raised in constant smoke exhibit RPE/BrM alterations including a thickening of BrM and lose contrast sensitivity in the optokinetic reflex (OKR) assay over time and, all dependent on alternative pathway of complement activation (Kunchithapautham et al., 2014; Woodell et al., 2013; Woodell et al., 2016). In addition, immunization of animals with cigarette-smoke modified elastin peptides augmented damage in an ox-elastin antibody formation dependent manner (Annamalai et al., 2020).

Here, mice were exposed to a peptide immunotherapy regimen (weekly; 1 [low dose, LD] or 10 μg [high dose, HD]) when compared to PBS controls and placed into the smoke chamber.

After 6 months of smoke exposure, ultrastructural differences in BrM were analyzed by EM (**Fig. 2**). As reported previously, smoke exposure leads to a thickening of BrM in particular in the outer collagenous layer (Annamalai et al., 2020; Woodell et al., 2013; Woodell et al., 2016), when compared to room air raised mice, albeit not uniformly. The extent of thickened BrM increased with smoke exposure in PBS injected mice when compared to controls (**Fig. 2A**). When analyzing percent damaged BrM and its size and width, a significant treatment effect was identified ($P<0.0001$), confirming an increase pathology in room air versus PBS treated mice ($P<0.05$), an effect that augmented in HD elastin PIT mice (PBS versus HD, $P<0.0001$) and

reduced in LD treated mice (room air versus LD, $P<0.005$). Specifically, the percent thickened BrM doubled from ~23% in room air mice to ~53% in PBS smoke exposed mice. While percent thickened BrM did not drop in the LD PIT mice (PBS versus HD, $P=0.73$), it significantly increased in the HD PIT mice to 87% (PBS versus LD, $P=0.002$; LD versus HD, $P<0.01$). However, the percent thickened BrM does not take the overall size and area of the deposits into account, which was assessed in multiple 10 μm sections. Together, there was a reduction following LD PIT (PBS versus LD, $P<0.005$), but an increase in HD PIT (LD versus HD: $P<0.0001$), and room air and LD samples were indistinguishable ($P=0.98$).

We have shown that C57B/6J mice lose contrast sensitivity as assessed by OKR when exposed to long-term smoke [19, 20, 23] and have assessed contrast thresholds here in PBS, LD- and HD-PIT smoke exposed animals (**Fig. S1**) assessing vision loss over time (**Fig. S1A**), mean contrast threshold (**Fig. S1B**), and start and endpoint comparison. PBS-injected mice exhibited threshold elevations over time (repeated measures ANOVA; $P<0.05$), which was reduced in LD-PIT mice (PBS-LD comparison, $P<0.05$), but not HD-PIT mice (PBS-HD comparison, $P=0.2$). Mean contrast threshold over time revealed a difference for the PBS-LD ($P=0.001$) but not the PBS-HD comparison (**Fig. 2B**). On the final day of measurement, OKR contrast sensitivity differed significantly from the 1 month value for the PBS ($P<0.002$) and the HD treatment group ($P<0.005$), but not the LD group ($P=0.1$).

Anti-elastin antibody production

Sera of the peptide immunotherapy and smoke exposed mice were analyzed for the level of anti ox-elastin IgG and IgM antibodies produced over time. ELISA measurements over 3 dilutions

using repeated measures ANOVA revealed an IgG by treatment (P<0.0001) and IgM by treatment effect (P<0.0001). IgG (P<0.0001) and IgM levels (P<0.0001) were significantly increased in PBS treated smoke-exposed animals when compared to room air controls (**Fig. 3A, B**). LD PIT significantly reduced the amount of anti-ox-elastin antibodies (IgG P<0.005, IgM P<0.005), whereas HD PIT increased those levels (IgG P<0.01, IgM P<0.01).

Lower levels of IgG1 in comparison with IgG2a are typically associated with protective immunity (Rostamian et al., 2017). Here we tested the amount of anti-ox-elastin IgG1 and IgG2a antibodies present in the sera of PIT mice, which revealed a IgG1 by treatment (P<0.001) and a IgG2a by treatment effect (P<0.001). IgG1 levels were significantly increased in smoke-exposed PBS injected animals when compared to room air controls (IgG1 P<0.001), the IgG2a levels almost reached significance (P=0.0089; Bonferroni requires P value to be less than 0.0083 to reach significance) (**Fig. 4A, B**), but on average, IgG1 and IgG2a levels were unaffected by LD or HD PIT (P>0.3). When assessing the IgG1/IgG2a ratio at the two higher serum concentrations for the ELISA, the ratio was increased in smoke-exposed PBS injected animals when compared to room air controls (P<0.001), but was not affected by PIT (**Fig. 4C**). Finally, IgE production has been shown to mediate inflammatory responses associated with allergies and be highly sensitive to oral tolerance. Again, anti-ox-elastin IgE levels revealed an IgE by treatment effect (P<0.001) (**Fig. S2**), with levels significantly elevated in smoke-exposed animals when compared to room air controls (P<0.001), an effect that was further augmented by PIT (P<0.001), but revealing no dose-dependent effect on IgE levels.

Peptide Immunotherapy with ox-elastin reduced ocular complement activation and IgG/IgM deposition upon smoke exposure

The modulation of anti-elastin antibody levels in serum in response to PIT and smoke exposure suggests that the amount of IgG and IgM deposition in the RPE/choroid previously reported in smoke-exposed animals (Annamalai et al., 2020) might be reduced. RPE/choroid samples were probed for the presence of IgG and IgM antibodies using quantitative Western blotting (**Fig. 5A**). Smoke exposure in the presence of PBS injections increased both IgG and IgM levels in the RPE choroid fraction when compared to room air (IgG: P=0.002; IgM: P<0.01, combined antibody response $P<0.0001$). LD PIT decreased the combined antibody response significantly ($P<0.01$), HD PIT had no effect ($P=0.8$) (**Fig. 5A**). The subclasses of IgG antibodies were not further analyzed.

To quantify complement activation in RPE/choroid of PIT mice, protein samples from the same samples as above were analyzed by quantitative western blotting. Blots were probed with an antibody against C3d that recognizes C3α breakdown products C3α', C3α'1, and C3dg that can be distinguished based on their molecular weights (**Fig. 5B**). All three products were significantly increased by smoke exposure in PBS injected animals when compared to room air controls (C3α': $P<0.01$; C3α'1: $P=0.001$, and C3dg: $P<0.0001$). LD PIT significantly reduced those levels (C3α': $P=0.02$; C3α'1: $P<0.01$, and C3dg: $P<0.005$). HD PIT in contrast significantly elevated levels of C3α'1 over those observed without PIT ($P=0.03$), but had no effect on the other two components. Overall, when analyzing the three parameters together, using a repeated measure ANOVA, a complement activation products by treatment effect could be confirmed ($P<0.0001$). Together, complement activation was increased by smoke (room air

versus smoke/PBS, *P*=0.002), decreased by LD PIT (smoke/PBS versus LD, *P*=0.03) to room air levels (room air versus LD, *P*=0.2), but not by HD PIT in smoke exposed animals (smoke/PBS versus HD, *P*=0.3).

Peptide immunotherapy with ox-elastin alters ocular cytokine levels upon smoke exposure

As a readout of the dysregulation in the balance of Th1 and Th2 responses, levels of cytokines associated with Th1 and Th2 responses were assessed to determine if local inflammation in the RPE/choroid fraction was perturbed. To this end, as a broad assessement, protein samples from the same samples as above were analyzed by quantitative western blotting for immunoregulatory cytokines TGFβ, IL-4, IL-10 and pro-inflammatory cytokine IFNγ were analyzed (**Fig. 6**). Smoke exposure in PBS injected animals was found to significantly increase IFNγ when compared to room air controls (*P*<0.001) (**Fig. 6D**), which was reduced by LD PIT (*P*<0.001) but not HD PIT. Smoke exposure lead to an increase in IL4 (*P*<0.05) (**Fig. 6B**), that was significantly augmented by LD PIT (*P*<0.05) but not by HD PIT. Relative levels of TGFβ were significantly increased by smoke (*P*<0.001), and further increased by PIT in a dose-dependent manner (smoke + PBS vs smoke + LD, P<0.05; smoke + LD vs smoke + HD, *P*<0.05) (**Fig. 6A**). Levels of IL-10 were significantly decreased by smoke (*P*<0.01), and not altered by PIT irrespective of dose (**Fig. 6C**).

DISCUSSION

The main results of the current study are: 1) Elimination of antibody signaling via Fcγ receptor activation prevented vision loss and structural damage, providing additional rational for the

peptide immunotherapy. 2) Low dose PIT mice produced a lower ox-elastin-specific IgG and IgM immune response, leading to reduced complement activation and IgG/IgM deposition in the RPE/choroid; 3) Reduced complement activation in the RPE/choroid was associated with a greater preservation of BrM structure and preservation of visual function; 4) Treatment with ox-elastin peptide altered the inflammatory milieu and was associated with reduced IFNγ and increased IL-4 in the RPE/choroid fraction. Taken together, our results support that in the SIOP model, reducing antibodies generated de-novo against ox-elastin following PIT with a mouse ox-elastin peptide reduces complement activation and inflammation in the RPE/choroid. PIT induced reduction of inflammation and tissue damage was accompanied by reduced levels of IFNγ and increased levels of IL-4 in the RPE/choroid fraction, although mechanisms of immune deviation have not been defined fully. Finally, our previous publication on the requirement of the complement system for SIOP damage together with the current observation that elimination of Fcγ receptors prevented pathology, suggests that both complement-dependent cytotoxicity and antibody-dependent cell-mediated cytotoxicity contribute to damage.

The mouse model of long-term smoke exposure has been proposed by Wang and Neufeld as a potential model for studying accumulation of drusen-like material on BrM as they showed C3a, C5, C5b-9 and CFH deposition as well as CD63 and αB cystallin in the area of BrM (Wang et al., 2009; Wang and Neufeld, 2010). We have shown that pathology in this mouse was dependent on activation of the AP of complement, as $fB^{-/-}$ were protected from developing pathology (Woodell et al., 2013), and an AP inhibitor was found accelerate recovery from SIOP, allowing for the removal deposits in BrM and reciovery of constrast sensitivity (Woodell et al., 2016). Smoke exposure was found to increase IgG and IgM leves, with IgG1, 2a, 2b and 3 all being elevated

(Annamalai et al., 2020). Our results using elastin versus ox-elastin immunization, in which we showed increased deposition of IgG, IgM and complement C3 acitvation products in RPE/choroid upon ox-elastin immunization suggests that anti-ox-elastin antibodies are pathogenic. Support for this hypothesis comes from studies examining the mouse model of emphysema in response to long-term smoke. Elastin fragments have been shown to be proinflammatory in cigarette smoke induced emphysema, as mice deficient in the macrophage elastase matrix metalloproteinase-12 do not develop disease (Aggarwal, 2006). And Patel and colleagues have shown that the increased levels of IgM/IgG autoantibodies are pathogenic by transplanting donor lungs into animals after 6 months of smoke exposure. Two days after transplantation, the donor lungs showed increased IgM, IgG and activated complement, exacerbating post-transplant ischemia reperfusion injury (Patel et al., 2019). Antibodies bound to their respective ligands on cell surfaces, basement membranes or extracellular matrices can tirgger pathology via CDC and ADCC. Contribution of CDC was already confirmed based on the results on the $fB^{-/-}$ data (Woodell et al., 2013) as well as unpublished data, demonstrating that $C3^{-/-}$ are likewise protected (Woodell and Rohrer, 2013). Contribution of ADCC was confirmed here demonstrating that a global knockout for FcγRIII on effector cells eliminated pathology. In support of a potential role of Fcγ receptor signaling, Murinello and colleagues have shown that mice immunized against ovalbumin developed immune complexes in the retina, that led to the recruitment of myeloid cells and increased expression of FcγR. Likewise, they found that early AMD was associated with deposition of IgG, C1q, and membrane attack complex in the choriocapillaris and with increased numbers of CD45+ cells expressing FcγR (Murinello et al., 2014). And while elucidation of the exact mechanisms of antibody-induced pathology remains outstanding, the data suggests that pathology may be reduced by peptide immunotherapy.

Peptide immunotherapy has been studied extensively for the treatment of autoimmune diseases, allergy and cancer with delivery routes for the antigens, ranging from oral, to nasal, skin, intravenous, intraperitoneal or intramuscular (Larche, 2014; Romano et al., 2019; Shakya and Nandakumar, 2018; Smith and Peakman, 2018). With this in mind a similar approach to reduce pathologic effect from neo-antigens generated in degenerative disease has merits. This aligns and in common with other inflammatory diseases even in absence of direct causal evidence of antigen-specific pathogenesis in man. The normal activity of peripheral tolerance prevents heightened immune responses to different environmental factors such as food, allergens (Wawrzyniak et al., 2017), environmental skin or lung exposure (Li and Boussiotis, 2008), or altered gut microbiome (Wu and Wu, 2012). Therapeutically, the exact mechanisms of immune modulation and suppression of disease is not fully defined (Sabatos-Peyton et al., 2010). Experimentally, and in broad terms, peripheral tolerance towards certain antigens can be achieved after repeated exposure that induces deletion of reactive T cells or induce T cell anergy and/or generation of regulatory T (Treg) cells which are heterogeneous in nature and function, largely IL2 dependent and TGFβ. TR1 cells that are specific against a given antigen produce in particular high levels of IL-10 , IL-35 and TGF-β (Levings and Roncarolo, 2000) and a subset of B regulatory cells that make IL-10 and TGF-β (Vadasz et al., 2013). Treg cells may have multiple actions including and not exclusively, inhibition of Th1 cells and reduction in activation of innate immune cells. This requires cell-contact-dependent and -independent mechanisms, the latter which includes the secretion of IL-10 and TGF-β. In addition, tolerance might include an altered response of macrophages to the repeated exposure to the antigen (Butcher et al., 2018); however we have not yet examined the number of choroidal macrophages in this model. We

419 have not here shown causality of ox-elastin antibodies in SIOP model pathology,
420 notwithstanding the evidence herein of attenuating disease with peptide immunotherapy and
421 being able to increase pathology by immunizing mice with peptide. Ultimately, to elucidate
422 pathogenesis and mechanisms, adoptive and passive transfer of T cells or specific ox-elastin
423 antibodies would certainly inform (as would utilizing $rag^{-/-}$ mice), abeit recognizing the challenge
424 of experimental design in a model requiring months to propagate pathology.
425
426 We wished to assess whether there was a therapeutic efficacy of peptide immunotherapy and
427 provide supportive evidence of concomitant changes in inflammation biomarkers, rather than
428 pathways. Hence, we did not assess the generation of Treg cells directly, but our data
429 demonstrates that with LD treatment that attenuates pathology was associated with reduced IFNγ,
430 increased TGFβ and altered ox-elastin antibody response and subsequent complement activation.
431
432 In age-related macular degeneration, ocular immune responses have been considered as a
433 possible long term therapeutic target for disease prevention (Nussenblatt et al., 2014). This
434 approach is based on the following considerations around immune senescence and inflamm-
435 ageing (Fulop et al., 2017). Age is the most significant risk factor for AMD, and there exist
436 alterations in innate and adaptive immune responses with aging. Those include alterations in
437 RPE function as well as activation and infiltration of innate immune cells into the ocular tissue,
438 resulting in a para-inflammatory microenvironment (Chen and Xu, 2015). Th17 cells have been
439 observed in AMD, activated and recruited by complement C5a in human tissues (Liu et al.,
440 2011) as well as animal models (Rohrer, 2016). In addition, AMD is correlated with elevated
441 levels of autoantibodies and the role of immune responses extensively reviewed (Ambati et al.,

2013). Those include retinal IgG autoantibodies such as the retinol binding protein 3 elevated in wet AMD and retinaldehyde binding protein 1 elevated in dry AMD (Morohoshi et al., 2012a), as well as an array of both IgG and IgM antibodies against epitopes know to be generated in AMD, but that are not specific to the eye (Morohoshi et al., 2012b). Antibodies binding to antigens in tissues provide one of the activators of complement, which might explain the presence of an overactive complement system in AMD (Hageman et al., 2001). Based on these observations, Nussenblatt and colleagues have suggested that AMD would be suitable for tolerance therapy, which would re-align the adaptive immune response by suppressing T cell responses (Nussenblatt et al., 2014). Unfortunately due to his untimely death, the hypothesis was never tested.

To assess biomarkers and evidence of reduced inflammation that parallels the positive clinical outcomes we have presented alongside the generation of anti-ox-elastin antibodies with smoke exposure, we note elevated levels of IgM, IgG (including IgG1 and IgG2) and IgE. In addition,, smoke exposure resulted in a proinflammatory RPE/choroid environment displayed as elevated levels of complement and IFNγ and a reduction in IL-10. Although complement activation in serum was not examined here, it is known that exposure to cigarette smoke leads to complement activation in serum (Robbins et al., 1991). C3d has been shown to act as a natural adjuvant, reducing the amount of antigen necessary to elicit an immune response, effects that are mediated through the activation of C3d-specific autoreactive memory T-cells (De Groot et al., 2015). In addition, C3d has been shown to stimulate antigen presentation by follicular dendritic cells and helps to maintain immunological B cell memory (Toapanta and Ross, 2006). Thus, smoke-induced complement activation may participate in the selection of antibodies against ox-elastin.

Irrespective of the dose of peptide immunotherapy, repeated exposure to the antigen led to a dose-dependent increase in the amount of serum IgG1, IgG2a and IgE antibodies, as well as a dose-dependent increase in the amount of TGFβ in the ocular tissues. These results represent a mixed response, as in mouse, production of IgG2a is representative of a Th1 response, IgG1 of a Th2 response (Berger, 2000). IgE antibody production tends to be associated with smoking (Kim et al., 2017) as well as hypersensitivity reactions (Corry and Kheradmand, 1999), and Th2 cytokines activate and recruit IgE antibody producing B cells (Deo et al., 2010). The role of TGF-β is to maintain tolerance by regulating lymphocyte proliferation, differentiation, and survival (Li et al., 2006).

The low dose of ox-elastin peptide immunotherapy was found to reduce the humoral response to ox-elastin represented by the levels of anti-ox-elastin IgM, IgG antibodies found in serum. Persistence of ox-elastin presentation to immune cells is thought to induce T-cell tolerance and reduce B-cell activation. This reduction in the anti-ox-elastin humoral response was associated with reduced levels of IgG and IgM deposited in the RPE/choroid fraction of the smoke-exposed eye as well as a reduction in complement activation, resulting in ameliorated structure and function loss. The cytokine changes that were unique to the low dose of peptide are reduced levels of IFNγ and increased levels of IL-4 in the RPE/choroid fraction. Overall, the biomarker assessment of increase in IgG1 with IL-4 and TGFβ supports a modulation of inflammation and the clinical attenuation of disease we noted.

Our study has a number of limitations. First, with respect to the treatment paradigm and animal

488 model, we did not test the effects of peptide immunotherapy in room air only mice, nor did we
489 include peptide immunotherapy in FcγR$^{-/-}$ mice. Peptide injections in naïve, room air mice might
490 have revealed potential cell surface elastin receptor-mediated effects (Skeie et al., 2012) that
491 would have been masked in our experiments. Also, the effects of smoke-exposure and treatment
492 on the eye cannot be distinguished from that of the effects of the two on other organs. Animals
493 exposed to long-term smoke develop emphysema and other organ damage (Vandivier and
494 Ghosh, 2017). In addition, due to the limitations of available tissues after long-term smoke
495 exposure, systemic T-cell responses were not established, nor could the sources of the cytokines
496 (invading immune cells or RPE cells) be established to further illuminate mechanisms. Of note,
497 RPE cells have been shown to release TGFβ (Klettner et al., 2019), whereas IL-10 (Idelson et al.,
498 2018), IFNγ (Jiang et al., 2013) and IL-4 (Baba et al., 2020) detection in the RPE
499 microenvironment is skewed to other cell types as shown through mRNA analysis in ARPE-19
500 cells (Sharma et al., 2005). Second, while the animal model share certain similarities with dry
501 AMD at the light microscopy level (Wang et al., 2009; Wang and Neufeld, 2010), the EM
502 analysis revealed that thickened BrM occurs in the outer, rather than the inner collagenous layer.
503 In the human eye, EL is thinner and less abundant in the macula than in the periphery, in
504 particular in eyes with early AMD and active CNV (Chong et al., 2005); and while EL thinning
505 is observed in the SIOP model, the animals do not progress to CNV within the study period
506 (Woodell et al., 2013). Here we showed that in the mouse, elevated levels of elastin peptide and
507 anti-ox-elastin IgG/IgM antibodies have been detected after smoke-exposure. In AMD, serum
508 elastin-peptide levels are elevated in AMD in a disease-severity-dependent manner (Sivaprasad
509 et al., 2005), and levels of α-elastin antibodies are elevated, however, for both IgG and IgM
510 autoantibodies only neovascular AMD exhibited elevated levels (Morohoshi et al., 2012b).

Pathogenic antibodies are generated against neoepitopes, hence without any knowledge of the neoepitope on elastin-fragments generated in aging and AMD, it is unclear as to the predicted role of the α-elastin IgG and IgM antibodies in neovascular AMD (Morohoshi et al., 2012b). Likewise, whether the serum elastin-peptides are oxidized and to what extent in AMD patients is unknown, a question that could be solved with tandem mass spectrometry.

In summary, AMD pathogenesis has been linked to smoking, complement activation and pathogenic T and B cell immunity, and so peptide or antigen immunotherapy to suppress immunity has gathered support as a therapy. Here we provide new data that show that peptide immunotherapy by low-dose elastin peptide modified by smoke can ameliorate functional and morphological defects at the posterior pole of the eye generated by smoke exposure, resulting in a reduction of complement activation. Our results may open a novel avenue for immunotherapies in dry AMD.

ACKNOWLEDGEMENTS

Funding for this project was provided in part by the National Institutes of Health (NIH) R01EY019320 (BR), R01EY015128 (BJ), R01EY028927 (BJ) and P30EY014800 (BJ), the Department of Veterans Affairs RX000444 and BX003050 (BR), the South Carolina SmartState Endowment (BR), and an Unrestricted Research Grant from Research to Prevent Blindness, New York, NY to the Department of Ophthalmology & Visual Sciences, University of Utah. ADD is supported in part through the National Institute for Health Research (NIHR) Biomedical Research Centre at Moorfields Eye Hospital and University College London Institute of

Ophthalmology. We would like to thank Carl Atkinson (Medical University of South Carolina) for the room air and smoke-exposed FcγR$^{-/-}$ mice.

ADD acts as a consultant for Novartis, Affybody, UCB, Hubble Tx and receives research grants from Janssen Pharmaceuticals and Meira GTX. All other authors have no financial conflicts of interest.

FIGURE LEGENDS

Figure 1. Fcγ receptor contribution to smoke-induced ocular pathology and vision loss. After 6 months of smoke or room air, FcγR$^{-/-}$ mice were assessed for visual function and histology. (**A**) Contrast threshold was assessed as described in Figure 1, in room air (control) and smoke exposed FcγR$^{-/-}$ mice, and found to be identical. (**B-D**) Electronmicroscopic images of room air and smoke-exposed mice were assessed. (**B**) Thickness of BrM, (**C**) and the structure of the basolaminar infoldings were unaffected by smoke exposure. (**D**) A representative electronmicroscopy image of each condition is provided. Data are expressed as mean ± SEM (n = 6 per condition in A, and multiple regions in 3 eyes per condition in B and C).

Figure 2. Ultrastructural changes in mice following smoke exposure and ox-elastin peptide immunotherapy (PIT).

Electron micrographs of the RPE/BrM/choriocapillaris complex (RPE/BrM/CC) obtained from C57BL/6J mice exposed to 6 months or room air were compared to those exposed to 6 months of smoke in the absence (smoke – PBS) and presence of LD-PIT or HD-PIT (smoke – LD-PIT; smoke – HD-PIT). **(A)** In a control animal raised in room air, BrM is smooth, with thickness ~0.22 μm. BrM in animals exposed to smoke exhibit thickening and development of deposits. BrM is similarly affected in mice treated with HD ox-elastin, compared to animals treated with LD ox-elastin, that looks closer to animals raised in room air when compared to mice that are smoke exposed but not treated with PIT. **(B)** The percent of thickened BrM (>0.28 μm) per stretch of tissue analyzed (set to 100% per section per animal) was significantly increased by smoke (P=0.03), unaltered by LD-PIT but increased by HD-PIT (P<0.01). (**C**) As the percent thickened BrM does not take the size (length and height) of the deposits into account, both were assessed and compared. The width and area of deposits was significantly increased by smoke (P<0.02), reduced to room air levels by LD-PIT (P=0.98) and augmented by HD-PIT (P<0.0001). Abbreviations: BrM, Bruch's membrane; BLI, basolaminar infoldings, RPE: retinal pigment epithelium. Data are expressed as mean ± SEM (multiple regions in 5-6 eyes per condition were analized in B and C)

Figure 3. Anti ox-elastin IgG and IgM antibody production in response to smoke, and modulation by peptide immunotherapy (PIT).

ELISA analysis was performed, coating plates with oxidized elastin peptide. Serum at different concentrations (1:100 to neat) from age-matched control animals (room air), animals exposed to smoke and treated with PBS, and smoke exposed animals treated with different doses of oxidized elastin were used to probe for binding, which was visualized with corresponding anti-mouse IgG

and IgM secondary antibodies. Values were background subtracted, averaged and plotted as mean ± SEM (n=3). After smoke exposure, a significant immune response against ox-elastin could be detected for both IgG and IgM, which was blunted by LD-PIT and augmented by HD-PIT.

Figure 4. Anti ox-elastin IgG1 and IgG2a antibody production in response to smoke, and modulation by peptide immunotherapy (PIT).

ELISA analysis was performed as described in Figure legend 3. Mouse antibody binding was visualized with corresponding anti-mouse IgG1 and IgG2a secondary antibodies; and values were background subtracted, averaged and plotted as mean ± SEM (n=3). (**A**) After smoke exposure, a significant immune response against ox-elastin could be detected for both IgG1 and IgG2a, which was augmented by ox-elastin peptide treatment in a dose-dependent manner. (**B**) The ratio of IgG1/IgG2a was increased in smoke-exposed animals when compared to control. However, there was no shift in ratio upon PIT.

Figure 5. Analysis of tissue IgG, IgM and complement products in response to smoke and ox-elastin peptide immunotherapy (PIT) in the RPE/choroid. (A) Equal amounts of RPE/choroid extracts (15 μg/lane) were loaded per lane, probed for mouse IgG (top blot) and IgM (middle blot), and band intensities quantified. Arbitrary values were established based on normalization with β-actin (bottom blot). Age-matched animals exposed to room air were compared to those raised in smoke and tolerized with different doses of oxidized elastin or PBS. IgG and IgM levels were elevated by smoke. LD-PIT reduced levels of IgG and IgM present in RPE/choroid, whereas HD-PIT had no effect. **(B)** Samples from the same RPE/choroid extracts

as in panel A (15 μg/lane) were loaded per lane, probed for C3d, and band intensities quantified. Arbitrary values were established based on normalization with β-actin. Age-matched animals exposed to room air were compared to those raised in smoke and immunized with control or oxidized elastin. C3β, C3dg and C3d levels were elevated in smoke-exposed animals. LD-PIT reduced levels of complement activation products present in RPE/choroid, whereas HD-PIT had little effect. Data are expressed as mean ± SEM (n = 3 independent samples per condition).

Figure 6. Analysis of Th1 and Th2 cytokines in response to smoke and ox-elastin peptide immunotherapy (PIT) in the RPE/choroid. Equal amounts of RPE/choroid extracts (15 μg/lane) were loaded per lane, probed with antibodies for different cytokines, and band intensities quantified. Arbitrary values were established based on normalization with β-actin. Age-matched animals exposed to room air were compared to those raised in smoke and treated with different doses of oxidized elastin or PBS. **(A)** TGFβ levels were elevated by smoke, and further increased by PIT in a dose-dependent manner. **(B)** IL-4 levels were elevated by smoke, and further increased by LD-PIT but not HD-PIT. (**C**) IL-10 levels were reduced by smoke, and unaffected by LD- or HD-PIT. (**D**) IFNγ levels were increased by smoke, reduced to control levels by LD-PIT and unaffected by HD-PIT. Data are expressed as mean ± SEM (n = 3 independent samples per condition).

References

Aggarwal, Y., 2006. Elastin fragments are pro‐inflammatory in the progression of emphysema. Thorax 61, 567-567.

626 Ambati, J., Atkinson, J.P., Gelfand, B.D., 2013. Immunology of age-related macular degeneration. Nat
627 Rev Immunol 13, 438-451.
628 Annamalai, B., Nicholson, C., Parsons, N., Stephenson, S., Atkinson, C., Jones, B., Rohrer, B., 2020.
629 Immunization Against Oxidized Elastin Exacerbates Structural and Functional Damage in Mouse Model
630 of Smoke-Induced Ocular Injury. Invest Ophthalmol Vis Sci 61, 45.
631 Baba, T., Miyazaki, D., Inata, K., Uotani, R., Miyake, H., Sasaki, S.I., Shimizu, Y., Inoue, Y., Nakamura, K.,
632 2020. Role of IL-4 in bone marrow driven dysregulated angiogenesis and age-related macular
633 degeneration. Elife 9.
634 Berger, A., 2000. Th1 and Th2 responses: what are they? BMJ 321, 424.
635 Blumenkranz, M.S., Russell, S.R., Robey, M.G., Kott-Blumenkranz, R., Penneys, N., 1986. Risk factors in
636 age-related maculopathy complicated by choroidal neovascularization. Ophthalmology 93, 552-558.
637 Brown, M.M., Brown, G.C., Stein, J.D., Roth, Z., Campanella, J., Beauchamp, G.R., 2005. Age-related
638 macular degeneration: economic burden and value-based medicine analysis. Can J Ophthalmol 40, 277-
639 287.
640 Butcher, S.K., O'Carroll, C.E., Wells, C.A., Carmody, R.J., 2018. Toll-Like Receptors Drive Specific Patterns
641 of Tolerance and Training on Restimulation of Macrophages. Front Immunol 9, 933.
642 Cameron, D.J., Yang, Z., Gibbs, D., Chen, H., Kaminoh, Y., Jorgensen, A., Zeng, J., Luo, L., Brinton, E.,
643 Brinton, G., Brand, J.M., Bernstein, P.S., Zabriskie, N.A., Tang, S., Constantine, R., Tong, Z., Zhang, K.,
644 2007. HTRA1 variant confers similar risks to geographic atrophy and neovascular age-related macular
645 degeneration. Cell Cycle 6, 1122-1125.
646 Chen, M., Xu, H., 2015. Parainflammation, chronic inflammation, and age-related macular degeneration.
647 J Leukoc Biol 98, 713-725.
648 Chong, N.H., Keonin, J., Luthert, P.J., Frennesson, C.I., Weingeist, D.M., Wolf, R.L., Mullins, R.F., Hageman,
649 G.S., 2005. Decreased thickness and integrity of the macular elastic layer of Bruch's membrane
650 correspond to the distribution of lesions associated with age-related macular degeneration. Am J Pathol
651 166, 241-251.
652 Corry, D.B., Kheradmand, F., 1999. Induction and regulation of the IgE response. Nature 402, B18-23.
653 Curcio, C.A., Johnson, M., 2013. Structure, Function, and Pathology of Bruch's Membrane . . London:
654 Elsevier, Inc.;, 465-481.
655 Curcio, C.A., Johnson, M., Rudolf, M., Huang, J.D., 2011. The oil spill in ageing Bruch membrane. Br J
656 Ophthalmol 95, 1638-1645.
657 De Groot, A.S., Ross, T.M., Levitz, L., Messitt, T.J., Tassone, R., Boyle, C.M., Vincelli, A.J., Moise, L., Martin,
658 W., Knopf, P.M., 2015. C3d adjuvant effects are mediated through the activation of C3d-specific
659 autoreactive T cells. Immunol Cell Biol 93, 189-197.
660 Deo, S.S., Mistry, K.J., Kakade, A.M., Niphadkar, P.V., 2010. Role played by Th2 type cytokines in IgE
661 mediated allergy and asthma. Lung India 27, 66-71.
662 Desai, D.D., Harbers, S.O., Flores, M., Colonna, L., Downie, M.P., Bergtold, A., Jung, S., Clynes, R., 2007.
663 Fc gamma receptor IIB on dendritic cells enforces peripheral tolerance by inhibiting effector T cell
664 responses. J Immunol 178, 6217-6226.
665 Elvington, M., Huang, Y., Morgan, B.P., Qiao, F., van Rooijen, N., Atkinson, C., Tomlinson, S., 2012. A
666 targeted complement-dependent strategy to improve the outcome of mAb therapy, and
667 characterization in a murine model of metastatic cancer. Blood 119, 6043-6051.
668 Fulop, T., Larbi, A., Dupuis, G., Le Page, A., Frost, E.H., Cohen, A.A., Witkowski, J.M., Franceschi, C., 2017.
669 Immunosenescence and Inflamm-Aging As Two Sides of the Same Coin: Friends or Foes? Front Immunol
670 8, 1960.
671 Hageman, G.S., Luthert, P.J., Victor Chong, N.H., Johnson, L.V., Anderson, D.H., Mullins, R.F., 2001. An
672 integrated hypothesis that considers drusen as biomarkers of immune-mediated processes at the RPE-

673 Bruch's membrane interface in aging and age-related macular degeneration. Prog Retin Eye Res 20, 705-
674 732.
675 Holers, V.M., 2003. The complement system as a therapeutic target in autoimmunity. Clin Immunol 107,
676 140-151.
677 Idelson, M., Alper, R., Obolensky, A., Yachimovich-Cohen, N., Rachmilewitz, J., Ejzenberg, A., Beider, E.,
678 Banin, E., Reubinoff, B., 2018. Immunological Properties of Human Embryonic Stem Cell-Derived Retinal
679 Pigment Epithelial Cells. Stem Cell Reports 11, 681-695.
680 Jiang, K., Cao, S., Cui, J.Z., Matsubara, J.A., 2013. Immuno-modulatory Effect of IFN-gamma in AMD and
681 its Role as a Possible Target for Therapy. J Clin Exp Ophthalmol Suppl 2, 0071-0076.
682 Johnson, M., Dabholkar, A., Huang, J.D., Presley, J.B., Chimento, M.F., Curcio, C.A., 2007. Comparison of
683 morphology of human macular and peripheral Bruch's membrane in older eyes. Curr Eye Res 32, 791-
684 799.
685 Jones, A., Kumar, S., Zhang, N., Tong, Z., Yang, J.H., Watt, C., Anderson, J., Amrita, Fillerup, H., McCloskey,
686 M., Luo, L., Yang, Z., Ambati, B., Marc, R., Oka, C., Zhang, K., Fu, Y., 2011. Increased expression of
687 multifunctional serine protease, HTRA1, in retinal pigment epithelium induces polypoidal choroidal
688 vasculopathy in mice. Proc Natl Acad Sci U S A 108, 14578-14583.
689 Kang, H.K., Michaels, M.A., Berner, B.R., Datta, S.K., 2005. Very low-dose tolerance with nucleosomal
690 peptides controls lupus and induces potent regulatory T cell subsets. J Immunol 174, 3247-3255.
691 Kim, Y.S., Kim, H.Y., Ahn, H.S., Sohn, T.S., Song, J.Y., Lee, Y.B., Lee, D.H., Lee, J.I., Jeong, S.C., Chae, H.S.,
692 Han, K., Yeo, C.D., 2017. The Association between Tobacco Smoke and Serum Immunoglobulin E Levels
693 in Korean Adults. Intern Med 56, 2571-2577.
694 Klettner, A.K., Dithmar, S., Detrick, B., Hooks, J.J., 2019. The RPE Cell and the Immune System. Retinal
695 Pigment Epithelium in Health and Disease, 101-114.
696 Kunchithapautham, K., Atkinson, C., Rohrer, B., 2014. Smoke Exposure Causes Endoplasmic Reticulum
697 Stress and Lipid Accumulation in Retinal Pigment Epithelium through Oxidative Stress and Complement
698 Activation. J Biol Chem 289, 14534-14546.
699 Larche, M., 2014. Mechanisms of peptide immunotherapy in allergic airways disease. Ann Am Thorac
700 Soc 11 Suppl 5, S292-296.
701 Levings, M.K., Roncarolo, M.G., 2000. T-regulatory 1 cells: a novel subset of CD4 T cells with
702 immunoregulatory properties. J Allergy Clin Immunol 106, S109-112.
703 Li, L., Boussiotis, V., 2008. Control and regulation of peripheral tolerance in allergic inflammatory
704 disease: therapeutic consequences. Chem Immunol Allergy 94, 178-188.
705 Li, M.O., Wan, Y.Y., Sanjabi, S., Robertson, A.K., Flavell, R.A., 2006. Transforming growth factor-beta
706 regulation of immune responses. Annu Rev Immunol 24, 99-146.
707 Lin, M.K., Yang, J., Hsu, C.W., Gore, A., Bassuk, A.G., Brown, L.M., Colligan, R., Sengillo, J.D., Mahajan,
708 V.B., Tsang, S.H., 2018. HTRA1, an age-related macular degeneration protease, processes extracellular
709 matrix proteins EFEMP1 and TSP1. Aging Cell 17, e12710.
710 Liu, B., Wei, L., Meyerle, C., Tuo, J., Sen, H.N., Li, Z., Chakrabarty, S., Agron, E., Chan, C.C., Klein, M.L.,
711 Chew, E., Ferris, F., Nussenblatt, R.B., 2011. Complement component C5a promotes expression of IL-22
712 and IL-17 from human T cells and its implication in age-related macular degeneration. J Transl Med 9, 1-
713 12.
714 Maclay, J.D., McAllister, D.A., Rabinovich, R., Haq, I., Maxwell, S., Hartland, S., Connell, M., Murchison,
715 J.T., van Beek, E.J., Gray, R.D., Mills, N.L., Macnee, W., 2012. Systemic elastin degradation in chronic
716 obstructive pulmonary disease. Thorax 67, 606-612.
717 Morohoshi, K., Ohbayashi, M., Patel, N., Chong, V., Bird, A.C., Ono, S.J., 2012a. Identification of anti-
718 retinal antibodies in patients with age-related macular degeneration. Exp Mol Pathol.

719 Morohoshi, K., Patel, N., Ohbayashi, M., Chong, V., Grossniklaus, H.E., Bird, A.C., Ono, S.J., 2012b. Serum
720 autoantibody biomarkers for age-related macular degeneration and possible regulators of
721 neovascularization. Exp Mol Pathol 92, 64-73.
722 Muller-Eberhard, H.J., 1988. Molecular organization and function of the complement system. Annu Rev
723 Biochem 57, 321-347.
724 Murinello, S., Mullins, R.F., Lotery, A.J., Perry, V.H., Teeling, J.L., 2014. Fcgamma receptor upregulation is
725 associated with immune complex inflammation in the mouse retina and early age-related macular
726 degeneration. Invest Ophthalmol Vis Sci 55, 247-258.
727 Nussenblatt, R.B., Lee, R.W., Chew, E., Wei, L., Liu, B., Sen, H.N., Dick, A.D., Ferris, F.L., 2014. Immune
728 responses in age-related macular degeneration and a possible long-term therapeutic strategy for
729 prevention. Am J Ophthalmol 158, 5-11 e12.
730 Patel, K.J., Cheng, Q., Stephenson, S., Allen, D.P., Li, C., Kilkenny, J., Finnegan, R., Montalvo-Calero, V.,
731 Esckilsen, S., Vasu, C., Goddard, M., Nadig, S.N., Atkinson, C., 2019. Emphysema-associated Autoreactive
732 Antibodies Exacerbate Post-Lung Transplant Ischemia-Reperfusion Injury. Am J Respir Cell Mol Biol 60,
733 678-686.
734 Rinaldi, M., Lehouck, A., Heulens, N., Lavend'homme, R., Carlier, V., Saint-Remy, J.M., Decramer, M.,
735 Gayan-Ramirez, G., Janssens, W., 2012. Antielastin B-cell and T-cell immunity in patients with chronic
736 obstructive pulmonary disease. Thorax 67, 694-700.
737 Robbins, R.A., Nelson, K.J., Gossman, G.L., Koyama, S., Rennard, S.I., 1991. Complement activation by
738 cigarette smoke. Am J Physiol 260, L254-259.
739 Rohrer, B., 2016. Connecting the innate and adaptive immune responses in mouse choroidal
740 neovascularization via the anaphylatoxin C5a and gammadeltaT-cells. Invest Ophthalmol Vis Sci 6, 23794.
741 Romano, M., Fanelli, G., Albany, C.J., Giganti, G., Lombardi, G., 2019. Past, Present, and Future of
742 Regulatory T Cell Therapy in Transplantation and Autoimmunity. Front Immunol 10, 43.
743 Rostamian, M., Sohrabi, S., Kavosifard, H., Niknam, H.M., 2017. Lower levels of IgG1 in comparison with
744 IgG2a are associated with protective immunity against Leishmania tropica infection in BALB/c mice. J
745 Microbiol Immunol Infect 50, 160-166.
746 Sabatos-Peyton, C.A., Verhagen, J., Wraith, D.C., 2010. Antigen-specific immunotherapy of autoimmune
747 and allergic diseases. Curr Opin Immunol 22, 609-615.
748 Saeed, A.F., Wang, R., Ling, S., Wang, S., 2017. Antibody Engineering for Pursuing a Healthier Future.
749 Front Microbiol 8, 495.
750 Shakya, A.K., Nandakumar, K.S., 2018. Antigen-Specific Tolerization and Targeted Delivery as
751 Therapeutic Strategies for Autoimmune Diseases. Trends Biotechnol 36, 686-699.
752 Sharma, R.K., Orr, W.E., Schmitt, A.D., Johnson, D.A., 2005. A functional profile of gene expression in
753 ARPE-19 cells. BMC ophthalmology 5, 25.
754 Sivaprasad, S., Chong, N.V., Bailey, T.A., 2005. Serum elastin-derived peptides in age-related macular
755 degeneration. Invest Ophthalmol Vis Sci 46, 3046-3051.
756 Skeie, J.M., Hernandez, J., Hinek, A., Mullins, R.F., 2012. Molecular responses of choroidal endothelial
757 cells to elastin derived peptides through the elastin-binding protein (GLB1). Matrix Biol 31, 113-119.
758 Smith, E.L., Peakman, M., 2018. Peptide Immunotherapy for Type 1 Diabetes-Clinical Advances. Front
759 Immunol 9, 392.
760 Stone, P.J., Gottlieb, D.J., O'Connor, G.T., Ciccolella, D.E., Breuer, R., Bryan-Rhadfi, J., Shaw, H.A.,
761 Franzblau, C., Snider, G.L., 1995. Elastin and collagen degradation products in urine of smokers with and
762 without chronic obstructive pulmonary disease. Am J Respir Crit Care Med 151, 952-959.
763 Thurman, J.M., Kulik, L., Orth, H., Wong, M., Renner, B., Sargsyan, S.A., Mitchell, L.M., Hourcade, D.E.,
764 Hannan, J.P., Kovacs, J.M., Coughlin, B., Woodell, A.S., Pickering, M.C., Rohrer, B., Holers, V.M., 2013.
765 Detection of complement activation using monoclonal antibodies against C3d. J Clin Invest 123, 2218-
766 2230.

Toapanta, F.R., Ross, T.M., 2006. Complement-mediated activation of the adaptive immune responses. Immunologic Research 36, 197-210.
Tom, I., Pham, V.C., Katschke, K.J., Jr., Li, W., Liang, W.C., Gutierrez, J., Ah Young, A., Figueroa, I., Eshghi, S.T., Lee, C.V., Kanodia, J., Snipas, S.J., Salvesen, G.S., Lai, P., Honigberg, L., van Lookeren Campagne, M., Kirchhofer, D., Baruch, A., Lill, J.R., 2020. Development of a therapeutic anti-HtrA1 antibody and the identification of DKK3 as a pharmacodynamic biomarker in geographic atrophy. Proc Natl Acad Sci U S A 117, 9952-9963.
Vadasz, Z., Haj, T., Kessel, A., Toubi, E., 2013. B-regulatory cells in autoimmunity and immune mediated inflammation. FEBS Lett 587, 2074-2078.
Vandivier, R.W., Ghosh, M., 2017. Understanding the Relevance of the Mouse Cigarette Smoke Model of COPD: Peering through the Smoke. Am J Respir Cell Mol Biol 57, 3-4.
Wang, A.L., Lukas, T.J., Yuan, M., Du, N., Handa, J.T., Neufeld, A.H., 2009. Changes in retinal pigment epithelium related to cigarette smoke: possible relevance to smoking as a risk factor for age-related macular degeneration. PLoS ONE 4, e5304.
Wang, A.L., Neufeld, A.H., 2010. Smoking mice: a potential model for studying accumulation of drusen-like material on Bruch's membrane. Vision Res 50, 638-642.
Wawrzyniak, M., O'Mahony, L., Akdis, M., 2017. Role of Regulatory Cells in Oral Tolerance. Allergy Asthma Immunol Res 9, 107-115.
Woodell, A., Coughlin, B., Kunchithapautham, K., Casey, S., Williamson, T., Ferrell, W.D., Atkinson, C., Jones, B.W., Rohrer, B., 2013. Alternative complement pathway deficiency ameliorates chronic smoke-induced functional and morphological ocular injury. PLoS ONE 8, e67894.
Woodell, A., Jones, B.W., Williamson, T., Schnabolk, G., Tomlinson, S., Atkinson, C., Rohrer, B., 2016. A Targeted Inhibitor of the Alternative Complement Pathway Accelerates Recovery From Smoke-Induced Ocular Injury. Invest Ophthalmol Vis Sci 57, 1728-1737.
Wu, H.J., Wu, E., 2012. The role of gut microbiota in immune homeostasis and autoimmunity. Gut Microbes 3, 4-14.

SUPPLEMENTAL MATERIAL

Supplemental Methods

Optokinetic Response Test. Visual acuity and contrast sensitivity of mice were measured under photopic conditions (mean luminance of 52 cd m^{-2}) by observing their optomotor responses to moving sine-wave gratings (OptoMotry) as previously described by us (Woodell et al., 2013). Since visual acuity does not change in response to smoke exposure (Woodell et al., 2013; Woodell et al., 2016), we only assessed contrast threshold at a fixed spatial frequency (0.131

cyc/deg) and speed (12 deg/s). Mice were analyzed monthly over the smoke exposure period, determining readouts at 1, 2, 3, 4 and 5 months.

ELISA assays. ELISA assays were performed as described in detail previously (Annamalai et al., 2020). Microtiter (Immulon2; Dynatech Laboratories, Chatilly, VA) plates were coated with 10 μg/mL cigarette smoke modified mouse lung elastin peptides, washed, blocked with 3% milk in PBS, followed by exposure to increasing doses of mouse serum (1:100 to neat) and probed with anti-mouse secondary antibodies (anti-IgE) coupled to peroxidase and color development using Turbo-TMB ELISA (Pierce; Thermo Scientific, Rockford, IL).

Supplemental Figure Legends

Figure S1. Peptide immunotherapy (PIT) with oxidized elastin impairs contrast sensitivity. Optomotor responses were analyzed over 5 months in C57BL/6J mice injected weekly with PBS or low dose (LD; 1 μg) or high dose (HD; 10 μg) smoke-modified oxidized elastin (ox-elastin). Contrast threshold was obtained at a fixed spatial frequency (0.131 cyc/deg) and speed (12 deg/sec). (**A**) Smoke exposed PBS treated mice showed a significant increase in the amount of contrast required to elicit a response. Mice with LD-PIT treatment had improved threshold responses whereas those with HD-PIT did not benefit from the treatment. (**B**) Mean contrast threshold of mice from panel **A** during the smoke-exposure period was assessed between the three groups. Contrast threshold was reduced by PIT in smoke-exposed mice in LD- but not HD-treatment. The OKR starting threshold is indicated (black line). Data are expressed as mean ± SEM (n = 5-9 per condition).

827 **Figure S2. Anti ox-elastin IgE antibody production in response to smoke, and modulation**
828 **by peptide immunotherapy (PIT)**.
829 ELISA analysis was performed as described in Figure legend 3. Mouse antibody binding was
830 visualized with corresponding anti-mouse IgE secondary antibody; and values were background
831 subtracted, averaged and plotted as mean ± SEM (n=3). After smoke exposure, a significant
832 immune response against ox-elastin could be detected for IgE, which was augmented by PIT
833 independent of dose.

PRECIS: Elastin-degradation in BrM in smoke-exposed mice is associated with generation of anti-elastin antibodies that bind to RPE-BrM, triggering complement activation. Treatment with smoke-modified elastin peptide reduces structural and functional damage, suggesting that AMD might be preventable.